WPS2-PR(17) 18250

J Loizu et al.

Equilibrium beta-limits in classical stellarators

Preprint of Paper to be submitted for publication in
Journal of Plasma Physics

This work has been carried out within the framework of the EUROfusion Consortium and has received funding from the Euratom research and training programme 2014-2018 under grant agreement No 633053. The views and opinions expressed herein do not necessarily reflect those of the European Commission.

Equilibrium β-limits in classical stellarators

J. LOIZU [1] †, **S. R. HUDSON** [2], **C. NÜHRENBERG** [1], **AND J. GEIGER** [1]

[1]Max-Planck-Institut für Plasmaphysik, D-17491 Greifswald, Germany

[2]Princeton Plasma Physics Laboratory, PO Box 451, Princeton, New Jersey 08543, USA

(Received 23 June 2017)

A numerical investigation is carried out to understand the equilibrium β-limit in a classical stellarator. The SPEC code is used in order to assess whether or not magnetic islands and stochastic field-lines can emerge at high β. Two modes of operation are considered: a *zero-net-current stellarator* and a *flux-conserving stellarator*. Despite the fact that relaxation is allowed, the former is shown to maintain good flux surfaces up to the equilibrium β-limit predicted by ideal-MHD, above which a separatrix forms. The latter, which has no ideal equilibrium β-limit, is shown to develop regions of magnetic islands and chaos at sufficiently high β, thereby providing a "non-ideal β-limit". Perhaps surprisingly, however, the value of β at which the Shafranov shift of the axis reaches a fraction of the minor radius follows *in all cases* the scaling laws predicted by ideal-MHD. We compare our results to the High-Beta-Stellarator theory of (Freidberg 2014) and derive a new robust prediction for the non-ideal equilibrium β-limit above which chaos emerges.

1. Introduction

In stellarators, the maximum achievable β is most probably set by the equilibrium and not by its stability (Helander *et al.* 2012). In fact, magnetic surfaces are not guaranteed to exist in three-dimensional MHD equilibria without a continuous symmetry (Meiss 1992). While stellarators can be designed to possess magnetic surfaces in vacuum (Hanson & Cary 1984; Cary & Hanson 1986; Hudson & Dewar 1997; Pedersen *et al.* 2016), the necessary existence of plasma currents that maintain force-balance at finite plasma pressure engenders the potential destruction of magnetic surfaces at sufficiently high β and can thus lead to the loss of confinement (Drevlak *et al.* 2005).

The equilibrium β-limit is not fully understood since it requires the accurate computation of three-dimensional MHD equilibria, which generally consist of an intricate combination of magnetic surfaces, magnetic islands, and magnetic field-line chaos. The Stepped-Pressure Equilibrium Code (SPEC) was developed as one possible approach to fulfil this highly non-trivial task (Hudson *et al.* 2012), although there are a few more ongoing complementary efforts (Suzuki *et al.* 2006; Hirshman *et al.* 2011). SPEC has been rigorously verified in axisymmetry (Hudson *et al.* 2012), in slightly perturbed configurations (Loizu *et al.* 2015*b*,*a*, 2016*a*), and more recently in stellarator geometries (Loizu *et al.* 2016*b*).

With a view to progressing towards an understanding of the β-limit in advanced, fusion-relevant stellarator experiments, we focus on a classical stellarator geometry with a simple pressure pedestal and perform a basic numerical study of its equilibrium β-limit. The simplified geometry allows us to use the High-Beta-Stellarator model (Freidberg 2014) to guide our investigation. This paper leads to the distinction between ideal and non-ideal

† Email address for correspondence: joaquim.loizu@ipp.mpg.de

equilibrium β-limits, for which we derive analytical expressions that push our theoretical understanding forward and validate the numerical calculations.

2. Model and control parameters

We consider the fixed-boundary problem of a finite β equilibrium in a classical $l = 2$ stellarator (Freidberg 2014). Namely, we must provide (i) the geometry of the boundary, e.g. via the Fourier coefficients of the cylindrical coordinates defining the boundary surface, $\{R_{mn}, Z_{mn}\}$; (ii) the pressure profile as a function of the enclosed toroidal magnetic flux, $p(\Psi)$; and (ii) an additional profile, e.g. the rotational transform, $\iota(\Psi)$, or the net toroidal current, $I_\varphi(\Psi)$.

2.0.1. *Boundary*

The simplest boundary representation that can model an $l = 2$ stellarator is that of a rotating ellipse with no toroidally averaged elongation. Namely,

$$\begin{aligned} R(\theta,\varphi) &= R_{00} + R_{10}\cos\theta + R_{11}\cos\left(\theta - N_p\varphi\right) \\ Z(\theta,\varphi) &= Z_{00} + Z_{10}\sin\theta + Z_{11}\sin\left(\theta - N_p\varphi\right) \end{aligned} \tag{2.1}$$

with $Z_{00} = 0$, $Z_{10} = -R_{10}$, and $Z_{11} = R_{11}$. For our β-limit study, the main parameters of interest in Eq. (2.1) are the major radius, R_{00}, and the number of field periods, N_p. In fact these can be used to vary independently the inverse aspect ratio, ϵ, and the vacuum rotational transform, ι_v, which are predicted to determine the ideal equilibrium β-limit. We therefore choose to fix the other parameters to $R_{10} = 1$ and $R_{11} = 0.25$. Two examples of such boundaries with different values of N_p are shown in Fig. 1.

The inverse aspect ratio is

$$\epsilon = \frac{r_{\text{eff}}}{R_{00}} \ , \tag{2.2}$$

where the effective minor radius is $r_{\text{eff}} = \sqrt{r_{\max} r_{\min}}$, with $r_{\max} = R_{10} + R_{11} = 1.25$ and $r_{\min} = R_{10} - R_{11} = 0.75$, respectively the major and minor axis of the rotating ellipse. The vacuum rotational transform can be estimated analytically (Helander 2014) as

$$\iota_v = \frac{N_p}{2}\frac{(r_{\max} - r_{\min})^2}{r_{\max}^2 + r_{\min}^2} \ . \tag{2.3}$$

For example, for $N_p = 5$ we get $\iota_v \approx 0.3$.

2.0.2. *Pressure profile*

We model a pressure pedestal by assuming that all the pressure gradient is concentrated on a single flux-surface, namely $p(\Psi) = p_0$ for $\Psi \leqslant \Psi_a$ and $p(\Psi) = 0$ for $\Psi \geqslant \Psi_a$. This step in the pressure is naturally described by the SPEC code: two Taylor-relaxed volumes (Taylor 1974) separated by an ideal-interface supporting a pressure step $[[p]] = p(\Psi_a^+) - p(\Psi_a^-) = p_0$, in correspondence to which a jump in B must arise according to $[[p + \frac{B^2}{2\mu_0}]] = 0$. This implies the presence of a surface current that is simply a weak representation of the pressure-driven (diamagnetic and Pfirsch-Schlüter) current. For our basic β-limit study, we choose to fix the value $\Psi_a = 0.3\Psi_{\text{edge}}$ and use the freedom in p_0 to control the value of β, which we define here as $\beta = 2\mu_0 p_0/B_0^2$, where $B_0 = B(\Psi = 0)$.

2.0.3. *Zero-net-current versus flux-conserving*

The SPEC code calculates MHD equilibria as extrema of the Multiregion, Relaxed MHD (MRxMHD) energy functional (Hole *et al.* 2007; Hudson *et al.* 2007). In essence, the

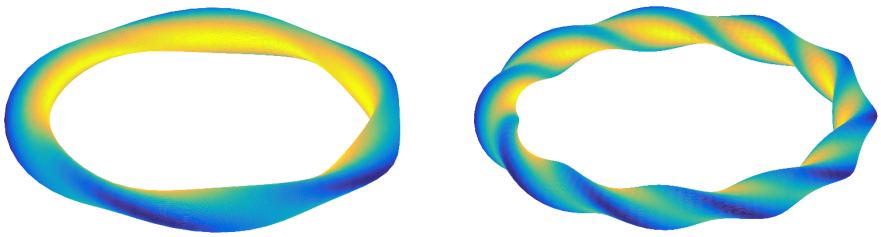

FIGURE 1. Boundary of a classical $l = 2$ stellarator with $N_p = 5$ (left) and $N_p = 10$ (right) field periods. The inverse aspect ratio is $\epsilon = 0.1$ and the colour represents the amplitude of the vacuum magnetic field on the boundary as computed from SPEC.

energy functional is the same as in conventional ideal MHD equilibrium theory (Kruskal & Kulsrud 1958), but the constraints under which the function is extremized are different. While in ideal-MHD the magnetic topology is *continuously* constrained, in MRxMHD the topology is only *discretely* constrained, thus allowing for partial relaxation. More precisely, the plasma is partitioned into a finite number, N_V, of nested volumes, V_v, that undergo Taylor relaxation. These volumes are separated by $N_V - 1$ interfaces that are constrained to remain magnetic surfaces during the energy minimization process. For the β-limit study at hand, we have $N_V = 2$ volumes separated by one ideal-interface. The location and shape of this interface is unkown *a priori* and determined self-consistently by a force-balance condition. MRxMHD equilibrium states satisfy

$$\nabla \times \mathbf{B} = \mu_v \mathbf{B} \quad \text{in the volumes} \tag{2.4}$$

$$\left[\left[p + \frac{B^2}{2\mu_0}\right]\right] = 0 \quad \text{on the interface} \tag{2.5}$$

for $v = 1, 2$. In addition to providing the enclosed toroidal fluxes in each volume (Ψ_a and Ψ_{edge}), the solution to Eq. (2.4) requires one more parameter if the volume is a topological torus (the innermost volume) and two more parameters if the volume is an annulus (the outer volume). Hence we must provide a total of 3 parameters to determine the equilibrium solution at a given value of β.

If we want to enforce a zero net-toroidal-current, $I_\varphi = 0$, we can impose $\mu_1 = \mu_2 = 0$ and then iterate on the total enclosed poloidal flux, ψ_p, until the surface current has no net toroidal component. At each iteration step, the net toroidal surface current can be easily calculated as

$$I_\varphi^{\text{CS}} = \int_0^{2\pi} [[\mathbf{B}]] \cdot \mathbf{e}_\theta \, d\theta \tag{2.6}$$

by virtue of Ampère's law. The iterative procedure can be implemented via a Newton method and brings I_φ^{CS} down to machine precision in a few steps. We refer to this mode of operation as *zero-net-current*.

If we want to constrain the rotational transform, $\iota(\Psi)$, we can enforce it to remain constant on both sides of the ideal-interface, $\iota_a^+ = \iota_a^- = \iota_a$, and at the edge, ι_{edge}. Once

again, this can be achieved by iterating on the values of $\mu_{1,2}$ and ψ_p. We refer to this mode of operation as *flux-conserving*.

We would like to remark that while the *zero-net-current* mode guarantees $I_\varphi = 0$, it does not guarantee that the rotational transform remains constant, and in particular we expect $\iota_a^+ \neq \iota_a^-$. Conversely, the *flux-conserving* mode guarantees that ι remains constant on certain surfaces (thus only locally flux-conserving) but in general we expect $I_\varphi \neq 0$, in particular at the location of the pressure-gradient.

3. High-β equilibria and Shafranov shift

Figure 2 shows Poincaré plots of the equilibirium magnetic field at different values of β for both the *zero-net-current* stellarator and the *flux-conserving* stellarator. In both cases there is a Shafranov shift that increases with β. However, the Shafranov shift of the axis, $\Delta_{\rm ax}$, increases with β much faster in the *zero-net-current* stellarator. It is useful to define the quantity

$$\beta_{0.5} \equiv \beta(\Delta_{\rm ax} = \frac{r_{\rm eff}}{2}) \ , \tag{3.1}$$

namely, the value of β at which the Shafranov shift of the axis reaches half of the minor radius. According to ideal-MHD equilibrium theory (Miyamoto 2005), $\beta_{0.5}$ is predicted to scale as

$$\beta_{0.5} \sim \epsilon\ \iota_v^2 \sim \frac{N_p^2}{R_{00}} \tag{3.2}$$

for large aspect ratios, $\epsilon \ll 1$, and slowly varying ι_v, which is true for $\iota_v \ll 1$. A scan in both R_{00} and N_p has been carried out in order to assess how $\beta_{0.5}$ scales in the numerical MHD calculations. Figure 3 shows the result of this scan. Despite the fact that SPEC allows for plasma relaxation, the scaling law (3.2) is very well reproduced in both modes of operation. However, the values of $\beta_{0.5}$ are much higher in the *flux-conserving* stellarator, by a factor of about 6. As we shall see now, this fundamental difference can be explained in terms of the High-Beta-Stellarator (HBS) model developed in (Freidberg 2014).

4. Ideal β-limit and the HBS theory

The HBS model for a classical stellarator developed in (Freidberg 2014) predicts that the rotational transform at the plasma edge, ι_a, evolves with β and plasma current as

$$\iota_a = (\iota_v + \iota_I)\left(1 - \nu^2\right)^{1/2} \tag{4.1}$$

where ι_I is the transform produced by the net toroidal current,

$$\iota_I = \frac{\mu_0 I_\varphi R_0}{2\pi a^2 B_0} \ , \tag{4.2}$$

and

$$\nu = \frac{\beta}{\epsilon_a(\iota_v + \iota_I)^2} \ , \tag{4.3}$$

where a is the effective minor radius of the plasma edge and $\epsilon_a = a/R$. For our system, we have $a = \sqrt{\Psi_a/\Psi_{\rm edge}} r_{\rm eff}$ and thus $\epsilon_a = \sqrt{\Psi_a/\Psi_{\rm edge}}\epsilon$.

In the context of the HBS theory, the *zero-net-current* stellarator can be analyzed by taking $\iota_I = 0$. Equation (4.1) then implies that ι_a decreases with increasing β. This is visible in Figure 4, where the profile $\iota(\Psi)$ obtained from SPEC at finite β is

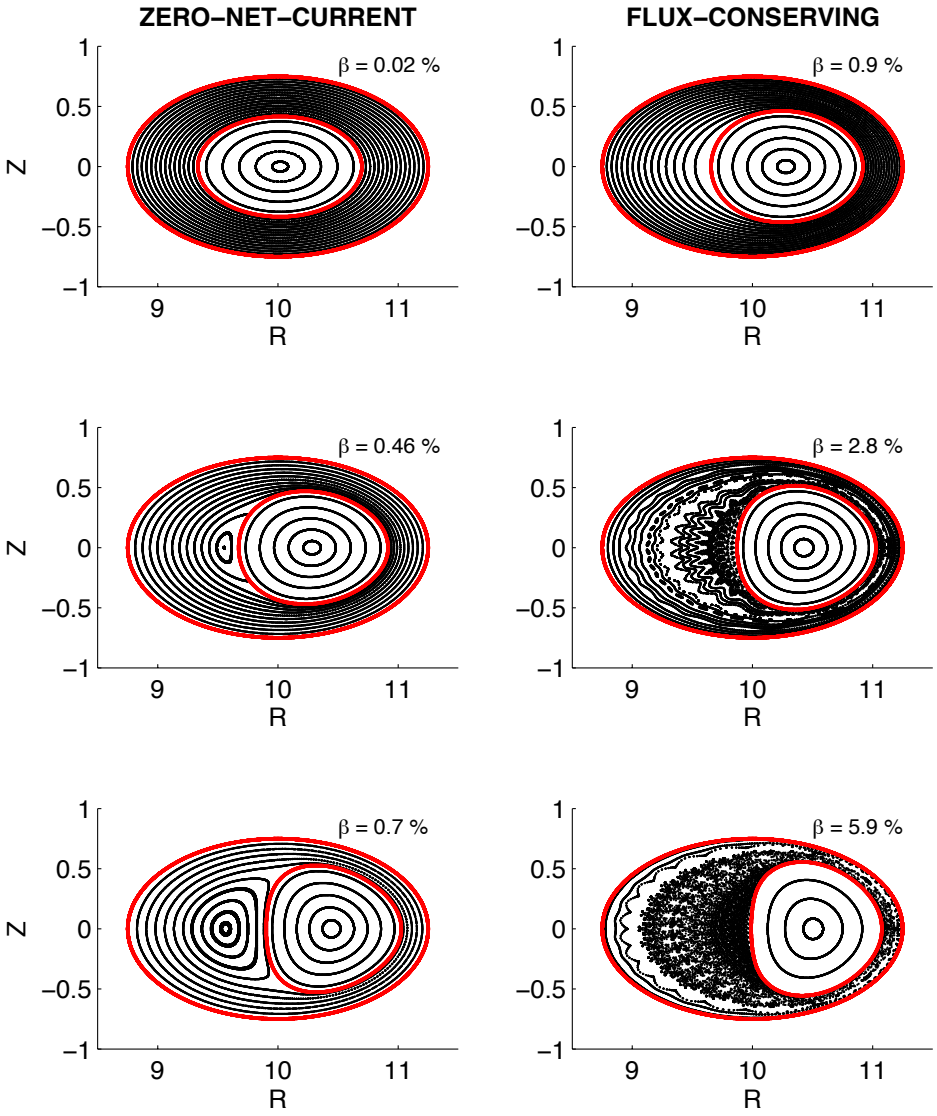

FIGURE 2. Poincaré section ($\varphi = 0°$) of the equilibrium magnetic field at different values of β. Left: *zero-net-current* stellarator. Right: *flux-conserving* stellarator. Here $N_p = 5$ and $\epsilon = 0.1$. Indicated in red are the boundary surface and inner interface supporting the pressure pedestal.

shown and compared to the vacuum transform. A jump in the rotational transform self-consistently develops on the ideal interface supporting the pressure gradient, namely at $\Psi_a = 0.3\Psi_{\text{edge}}$. The ideal MHD equilibrium code VMEC (Hirshman & Whitson 1983) was also run for this case with a pressure pedestal of small but finite width (the calculation requires a rather hight radial resolution, with about 3000 flux surfaces) and shown to produce essentially the same transform profile.

In Fig. 5, the value of ι_a is shown as a function of β and compared to the HBS prediction, Eq. (4.1), showing fairly good agreement (notice that there are no free parameters).

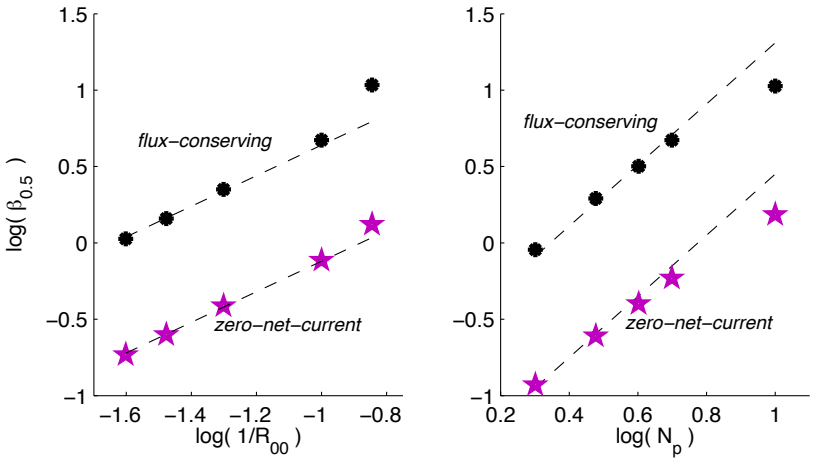

FIGURE 3. Scaling of $\beta_{0.5}$ with the inverse aspect ratio, $\epsilon \sim 1/R_{00}$ (left), and with the vacuum iota, $\iota_v \sim N_p$ (right). Black stars are for the *flux-conserving* stellarator. Magenta pentagrams are for the *zero-net-current* stellarator. The dashed lines have slope 1 (left) and 2 (right).

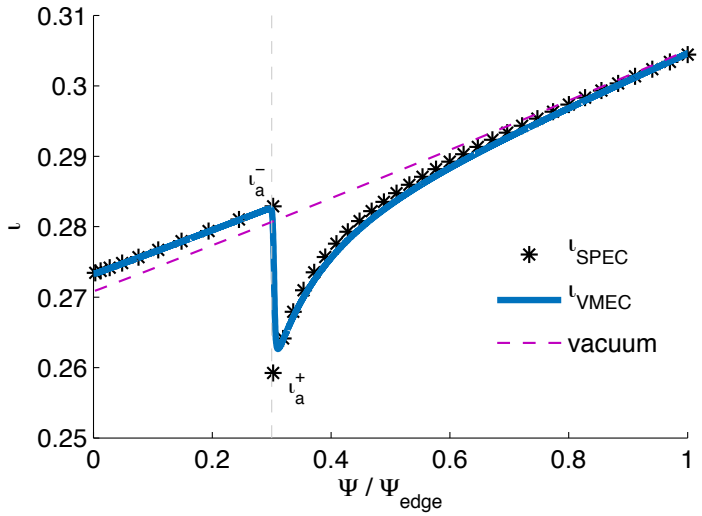

FIGURE 4. Rotational transform as a function of toroidal magnetic flux from both SPEC (black stars) and VMEC (solid blue line) at $\beta = 0.15\%$. For comparison, the vacuum transform is also shown (dashed magenta line). Here $N_p = 5$, $\epsilon = 0.1$, and the vertical dashed line indicates the location of the pressure pedestal.

The point where $\iota_a = 0$, which from Eq. (4.1) happens when $\nu = 1$, corresponds to the emergence of a separatrix (see, e.g., Fig. 2) and this defines the ideal β-limit, namely

$$\beta_{lim} = \epsilon_a \iota_v^2 \ . \tag{4.4}$$

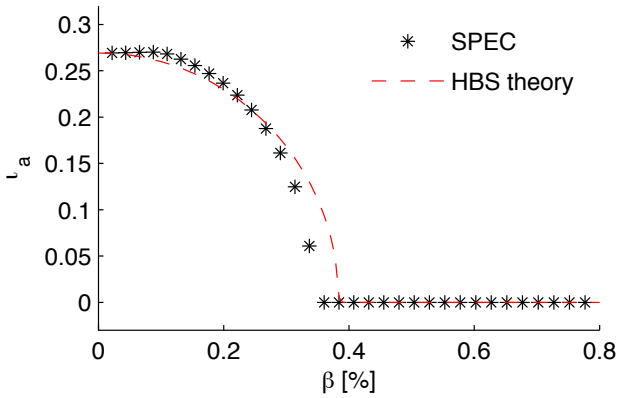

FIGURE 5. Rotational transform at the plasma edge, $\iota_a^+ = \iota(\Psi_a^+)$, as a function of β, from SPEC (black stars) and from Eq. (4.1) (dashed red line). Here $N_p = 5$ and $\epsilon = 0.1$.

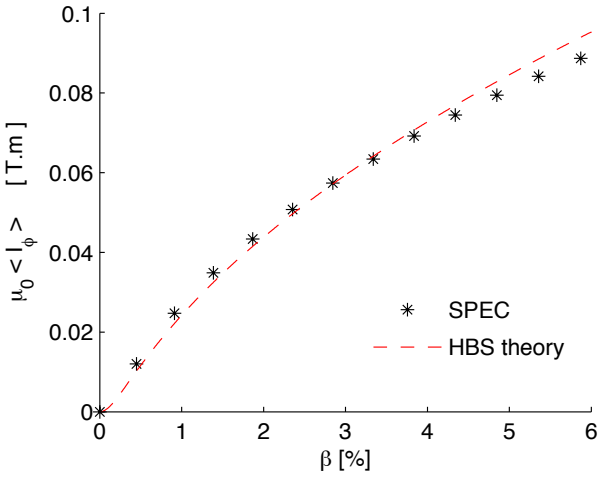

FIGURE 6. Net toroidal plasma current as a function of β, from SPEC calculations (black stars) and from Eq. (4.5) (dashed red line). Here $N_p = 5$ and $\epsilon = 0.1$.

For example, for the case depicted in Fig. 5 we have $\epsilon_a \approx 0.05$ and $\iota_v \approx 0.27$, thus Eq. (4.4) gives $\beta_{lim} \approx 0.4\%$, in good agreement with the SPEC calculations.

For the *flux-conserving* stellarator, we can impose $\iota_a = \iota_v$ in the HBS model. This leads to an expression for the value of the plasma current that is necessary to maintain ι_a constant. One obtains (Freidberg 2014)

$$\iota_I = \iota_v \left(\sqrt{\frac{1}{2}\left(1 + \sqrt{1 + 4H^2}\right)} - 1 \right) , \tag{4.5}$$

where

$$H = \frac{\beta}{\epsilon_a \iota_v^2} . \tag{4.6}$$

Figure 6 shows the net toroidal surface-current, I_φ, self-consistently generated in SPEC

equilibria as a function of β and compares it to the HBS prediction, Eq. (4.5), showing good agreement (again, there are no free parameters). For large $H \gg 1$, one has $I_\varphi \sim \sqrt{\beta}$, and the HBS model predicts that no β-limit is reached because the plasma current keeps rising and preventing the separatrix to form. From SPEC equilibrium calculations, however, where plasma relaxation is allowed, we observe that magnetic islands and chaotic field-lines emerge at sufficiently high β, thereby providing a "non-ideal β-limit".

5. Non-ideal β-limit and emergence of chaos

We can quantify the emergence of chaos by calculating the fractal dimension of the field-lines on the Poincaré section as a function of β (Meiss 1992). More precisely, we can evaluate the so-called *box-counting* dimension, or *Hausdorff* dimension,

$$D = \lim_{L\to 0} \left| \frac{\log(N)}{\log(L)} \right| \tag{5.1}$$

where L is the size of the boxes and N is the number of boxes containing at least one point of the magnetic field-line on the Poincaré section. If the field-line traces a magnetic surface, or even a magnetic island, one expects $D = 1$. If the magnetic field-line trajectory is chaotic, however, it fills up a certain "area" in the Poincaré section, and $D > 1$ is expected. We remark that the accurate evaluation of D requires a large number of toroidal transits, N_{trans}, when generating the Poincaré section via field-line-tracing. Satisfactory convergence was found at values of about $N_{trans} > 2 \times 10^4$.

Figure 7 shows the calculated fractal dimension as a function of the toroidal flux in equilibria of increasing β. First, we observe that for sufficiently low β we obtain $D(\Psi) = 1$, as expected, because magnetic surfaces are preserved in the entire volume. Second, we notice that for sufficiently high β there are regions in which $D(\Psi) > 1$ for $\Psi > \Psi_a$. Third, the value of D seems to be almost-binary, taking values at either $D \approx 1$ or $D \approx 1.6$. Fourth, the regions with $D \approx 1.6$ correspond to what appears to be stochastic regions in the corresponding Poincaré section. Finally, the volume occupied by these regions increases with β. These observations suggest that D is a good proxy for the emergence of chaos, which greatly simplifies the task of probing the "non-ideal β-limit". In fact, we can now define the volume of chaos, V_{chaos}, in the system as

$$V_{chaos} = V_{tot} \sum_{i=1}^{n_{lines}} \frac{(\Psi_i - \Psi_{i-1})}{\Psi_{edge}} \mathcal{H}(D(\Psi_i) - D_{crit}) \tag{5.2}$$

where V_{tot} is the total volume defined by the fixed-boundary, n_{lines} is the number of traced field-lines, $\Psi_i - \Psi_{i-1}$ measures the enclosed toroidal flux between two neighbouring field lines, and $\mathcal{H}$ is the Heaviside function, with $\mathcal{H} = 0$ for $D < D_{crit} = 1.5$ and $\mathcal{H} = 1$ otherwise. Figure 8 shows the profile of $V_{chaos}(\beta)$ calculated for two different values of N_p. Clearly, the emergence of chaos occurs at some critical value of $\beta = \beta_{chaos}$, which we define as the non-ideal equilibrium β-limit. The question remains: can we theoretically predict the value of β_{chaos}?

At this point we make the following hypothesis: the emergence of chaos shall occur when the perturbations in the poloidal field due to finite toroidal current are comparable to the vacuum poloidal field. Namely, chaos may emerge when $\iota_I(\beta) \sim \iota_v$. From the HBS theory we know that ι_I increases with β according to Eq. (4.5), hence applying our constraint we have

$$1 = \sqrt{\frac{1}{2}\left(1 + \sqrt{1 + 4\frac{\beta_{chaos}^2}{\epsilon_a^2 \iota_v^4}}\right)} - 1 \tag{5.3}$$

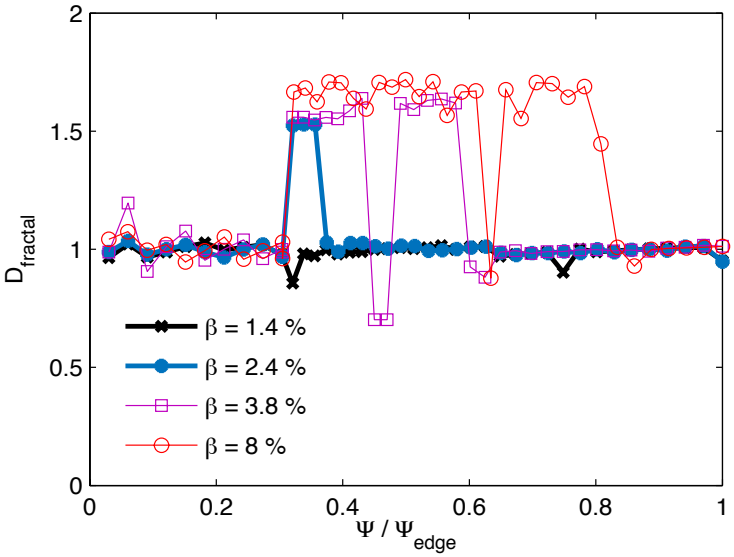

FIGURE 7. Fractal dimension of the magnetic field lines in a Poincaré section as a function of toroidal flux. The pressure pedestal is at $\Psi/\Psi_{edge} = 0.3$. Different curves are for different values of β. All equilibria have $N_p = 5$ and $\epsilon = 0.1$.

and hence

$$\beta_{chaos} = \sqrt{12}\epsilon_a \iota_v^2 \tag{5.4}$$

which gives $\beta_{chaos} \approx 0.5\%$ for $N_p = 3$ and $\beta_{chaos} \approx 1.4\%$ for $N_p = 5$, thus in excellent agreement with the observed transition to chaos (see Fig.8). More importantly, Eq. (5.4) is a general result and predicts that the non-ideal equilibrium β-limit scales exactly as the ideal equilibrium β-limit but with a larger factor in front, of the order of $\sqrt{12} \approx 3.5$.

6. Discussion

The equilibrium β-limit in a classical stellarator has been thoroughly investigated via numerical calculations that have guided our analytical understanding. A classical stellarator with zero net-toroidal-current possesses an equilibrium β-limit as predicted by ideal MHD, $\beta_{lim} = \epsilon_a \iota_v^2$, above which a separatrix forms due to the vanishing of the rotational transform at the plasma edge, $\iota_a \to 0$. A classical stellarator with constant ι_a, however, has a larger equilibrium β-limit that is of non-ideal nature. In fact, ι_a can be maintained at any value of β as long as a net-toroidal-current flows in the vicinity of the pressure pedestal; when such current produces a change in transform that is comparable to the vacuum transform, $\iota_I \sim \iota_v$, magnetic field-line chaos emerges in maximally-relaxed equilibria, and this occurs at $\beta_{chaos} = \sqrt{12}\epsilon_a \iota_v^2$. For $\beta > \beta_{chaos}$, the volume of destroyed magnetic surfaces increases monotonically with β and radially outward from the location of the pressure pedestal. We remark that this non-ideal β-limit does not consider the possibility of island-healing mechanisms; on the contrary, it considers the "worst-case-scenario" of complete relaxation. Therefore β_{chaos} should be interpreted as a lower bound for the β-limit of a classical stellarator where a net-toroidal-current clamps the value of ι_a. Furthermore, we would like to notice that a relatively small toroidal current is enough to maintain ι_a constant and therefore to raise the β-limit. For example, for a classical

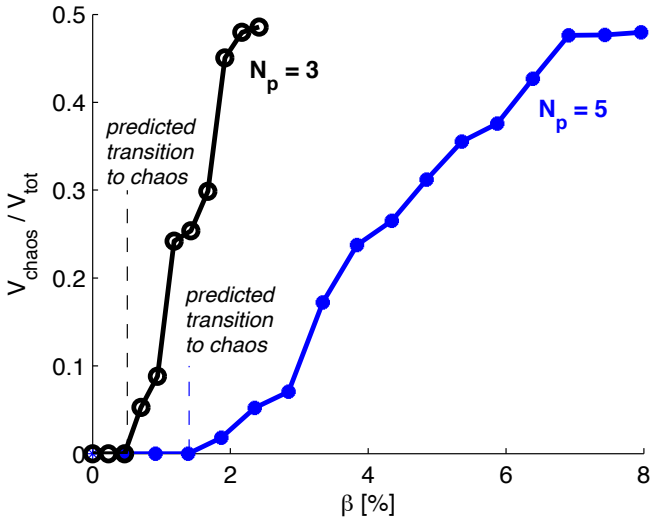

FIGURE 8. Volume of chaos as a function of β for $N_p = 3$ and $N_p = 5$ and fixed $\epsilon = 0.1$. The vertical dashed lines indicate the predicted transition to chaos at $\beta = \beta_{chaos}$ given by Eq. (5.4).

stellarator with $N_p = 5$, $\epsilon = 0.1$, $B_0 \sim 1$ T, and $R_0 = 10$ m, we have $I_\varphi \approx 40$ kA at about $\beta \approx 2\%$ (Fig. 6).

Two questions remain to be investigated: (1) can this predictive theory be extended to more complex stellarator geometries? (2) how to incorporate the possibility of pressure-induced island healing (Bhattacharjee *et al.* 1995; Narushima *et al.* 2008; Hegna 2012) in the derivation of the equilibrium β-limit? Some new ideas are here needed.

The authors would like to thank Per Helander, Sam Lazerson, and Jürgen Nührenberg for useful discussions. This work has been carried out in the framework of the EUROfusion Consortium and has received funding from the Euratom research and training programme 2014-2018 under Grant Agreement No. 633053. The views and opinions expressed herein do not necessarily reflect those of the European Commission.

REFERENCES

Bhattacharjee, A., Hayashi, T., Hegna, C. C., Nakajima, N. & Sato, T. 1995 Theory of pressure-induced islands and self-healing in three-dimensional toroidal magnetohydrodynamic equilibria. *Physics of Plasmas* **2** (3), 883.

Cary, John R & Hanson, J D 1986 Stochasticity reduction. *Physics of Fluids* **29**.

Drevlak, M, Monticello, D. & Reiman, A. 2005 PIES free boundary stellarator equilibria with improved initial boundary conditions. *Nuclear Fusion* (45), 731–740.

Freidberg, J P 2014 *ideal MHD*. Cambridge University Press.

Hanson, James D & Cary, John R 1984 Elimination of stochasticity in stellarators. *Physics of Fluids* **27**.

Hegna, C. C. 2012 Plasma flow healing of magnetic islands in stellarators. *Physics of Plasmas* **19** (5).

Helander, P. 2014 Theory of plasma confinement in non-axisymmetric magnetic fields. *Reports on Progress in Physics* **77** (8), 087001.

Helander, P, Beidler, C D, Bird, T M, Drevlak, M, Feng, Y, Hatzky, R, Jenko, F, Kleiber, R, Proll, J H E, Turkin, Yu & Xanthopoulos, P 2012 Stellarator and tokamak plasmas: a comparison. *Plasma Physics and Controlled Fusion* **54** (12), 124009.

Hirshman, S. P., Sanchez, R. & Cook, C. R. 2011 SIESTA: A scalable iterative equilibrium solver for toroidal applications. *Physics of Plasmas* **18** (6).

Hirshman, S P & Whitson, J C 1983 Steepest-descent moment method for three-dimensional magnetohydrodynamic equilibria. *Physics of Fluids* **26** (1), 3553–3568.

Hole, M.J, Hudson, S.R & Dewar, R.L 2007 Equilibria and stability in partially relaxed plasmavacuum systems. *Nuclear Fusion* **47** (8), 746–753.

Hudson, S R & Dewar, R L 1997 Manipulation of islands in a heliac vacuum field. *Physics Letters, Section A: General, Atomic and Solid State Physics* **226**, 85–92.

Hudson, S. R., Dewar, R. L., Dennis, G., Hole, M. J., McGann, M., Von Nessi, G. & Lazerson, S. 2012 Computation of multi-region relaxed magnetohydrodynamic equilibria. *Physics of Plasmas* **19** (11).

Hudson, S. R., Hole, M. J. & Dewar, R. L. 2007 Eigenvalue problems for Beltrami fields arising in a three-dimensional toroidal magnetohydrodynamic equilibrium problem. *Physics of Plasmas* **14** (5).

Kruskal, M. D. & Kulsrud, R. M. 1958 Equilibrium of a Magnetically Confined Plasma in a Toroid. *Physics of Fluids* **1** (4), 265.

Loizu, J., Hudson, S., Bhattacharjee, A. & Helander, P. 2015*a* Magnetic islands and singular currents at rational surfaces in three-dimensional magnetohydrodynamic equilibria. *Physics of Plasmas* **22** (2).

Loizu, J., Hudson, S. R., Bhattacharjee, A., Lazerson, S. & Helander, P. 2015*b* Existence of three-dimensional ideal-magnetohydrodynamic equilibria with current sheets. *Physics of Plasmas* **22** (9), 090704.

Loizu, J., Hudson, S. R., Helander, P., Lazerson, S. A. & Bhattacharjee, A. 2016*a* Pressure-driven amplification and penetration of resonant magnetic perturbations. *Physics of Plasmas* **23** (5).

Loizu, J., Hudson, S. R. & Nührenberg, C. 2016*b* Verification of the SPEC code in stellarator geometries. *Physics of Plasmas* **23** (11).

Meiss, J. D. 1992 Symplectic maps, variational principles, and transport. *Reviews of Modern Physics* **64** (3), 795–848.

Miyamoto, K 2005 *Plasma Physics and Controlled Nuclear Fusion*. Berlin: Springer-Verlag.

Narushima, Y., Watanabe, K.Y., Sakakibara, S., Narihara, K., Yamada, I., Suzuki, Y., Ohdachi, S., Ohyabu, N., Yamada, H. & Nakamura, Y. 2008 Dependence of spontaneous growth and suppression of the magnetic island on beta and collisionality in the LHD. *Nuclear Fusion* **48** (7), 075010.

Pedersen, T. Sunn, Otte, M., Lazerson, S., Helander, P., Bozhenkov, S., Biedermann, C., Klinger, T., Wolf, R. C., Bosch, H. S. & The Wendelstein 7-X Team 2016 Confirmation of the topology of the Wendelstein 7-X magnetic field to better than 1:100,000. *Nature Communications* **7**, 13493.

Suzuki, Yasuhiro, Nakajima, Noriyoshi, Watanabe, Kiyomasa, Nakamura, Yuji & Hayashi, Takaya 2006 Development and application of HINT2 to helical system plasmas. *Nuclear Fusion* **46** (11), L19–L24.

Taylor, J. B. 1974 Relaxation of toroidal plasma and generation of reverse magnetic fields. *Physical Review Letters* **33** (19), 1139–1141.